Coordinated Longitudinal and Lateral Control of Autonomous Electric Vehicles in a Platoon

Conference Paper · September 2016

DOI: 10.4271/2016-01-1875

1 author:

Jinghua Guo
Xiamen University
30 PUBLICATIONS **152** CITATIONS

SEE PROFILE

SAE INTERNATIONAL®

Coordinated Longitudinal and Lateral Control of Autonomous Electric Vehicles in a Platoon

2016-01-1875

Published 09/14/2016

Jinghua Guo
Xiamen University

CITATION: Guo, J., "Coordinated Longitudinal and Lateral Control of Autonomous Electric Vehicles in a Platoon," SAE Technical Paper 2016-01-1875, 2016, doi:10.4271/2016-01-1875.

Abstract

The studies of coordinated control method for autonomous electric vehicles face two major challenges such as: I) Autonomous electric vehicles have the properties of uncertain nonlinearities and strong coupling, the platoon control system should effectively overcome these characteristics. II) Over-actuated tire actuators are equipped with in the autonomous electric vehicles to improve the system reliability, and reconfigurablity, the platoon control system should real-time handle the redundancy of tire actuators. This paper presents a novel nonlinear coordinated control scheme aimed at the improvement of the automatic driving performance of multiple autonomous electric vehicles in a platoon. First, a nonlinear mathematic model which perfectly describes the dynamic behaviors of autonomous electric vehicles is deduced using Newton-Euler theorem. Secondly, an adaptive coordinated control scheme is designed to manage the longitudinal and lateral motion of vehicles, which is a double level control framework. An adaptive backstepping sliding mode high-level control law is presented to determine the total forces and torque of vehicles, the uncertainties and switching function terms are accurately regulated by the neuro network. Third, a dynamic coordinated low-level control law is proposed, a SQP control allocation algorithm, which can achieve the fault tolerance and reconfiguration of the redundant tire actuation system, is presented to generate the desired longitudinal and lateral tire forces. Then, the dynamic regulators consisting of an inverse tire model and two inner loops for each wheel is designed to achieve its desired forces. Finally, simulation results illustrate that the presented coordinated control scheme has the excellent tracking properties under different driving conditions..

Introduction

Autonomous distributed electric vehicles have drawn ex-tensive concern since they are considered to be safe and effective approaches that can sufficiently resolve these serious social problems such as traffic congestion, traffic safety and air pollution [1]. Formation control is regarded as one of the important issues of autonomous vehicles in intelligent transportation system (ITS), which is devoted to ensure that two or more autonomous vehicles travel in the same lane at the same speed with the desired inter-vehicle distances between any vehicle and its neighbors. The major advantages of the vehicle formation control system are increased safety and highway capacity.

The formation control problem is to find a scheme for autonomous vehicles such that they could keep a safe dis-tance from each other in a formation while tracking the desired reference trajectory. Since autonomous vehicles have the features of strong coupling, nonlinearities and parametric uncertainties, how to design the vehicle formation control approach is regarded as is a challenging task and has profound research significance.

Currently, more and more attentions are paid to the re-search theme of the formation control of autonomous vehicles in ITS. For instance, a possible framework for analyzing safety aspects of heavy duty vehicle platooning is presented in [2], the system states of two neighboring vehicles are conveyed through radar information and wireless communication, and the minimum safe spacing is studied for heterogeneous platoons. Ploeg et al.[3] employs a using a novel vehicle following control approach to increase the road throughput by a small intervehicle time gap, and the disturbance attenuation along the vehicle string is considered an essential requirement for the design of those systems. To achieve a satisfactory vehicle longitudinal speed regulation, Khalid et al. [4] develops a backstepping controller is developed to deal with the changing aerodynamics efforts and road slope. In [5], considering the negative effect of the tracking lag parameter, a hierarchical decentralized control of a platoon of vehicles with heterogeneous information feedback is established. Yue et al. [6] proposes a robust nonlinear control design method based on a disturbance observer and the backstepping technique, and the platoon control performance with a guaranteed level of attenuation of the disturbance is enhanced. Zhou et al. [7] designs a decentralized model predictive control approach to deal with the high latency in wireless communications and im-prove traffic safety.

It is known, however, that vehicles in a formation have the properties of external disturbances, uncertain nonlinearities and strong coupling, and their lateral and longitudinal coupled dynamic effects become increasingly significant as maneuvers involving larger tire forces, reduced road friction and higher accelerations.

In order to achieve the dynamic coupling compensation and improve the control performance, some efforts have attempted to combine longitudinal and lateral dynamic control for autonomous vehicles in a platoon. In[8,9], a nonlinear model-based predictive controller for combined lateral and longitudinal motion of autonomous vehicles is designed, in which a reference speed profile generator is adopted by taking account of the road geometry information, such that the lateral stability is guaranteed and the longitudinal control performance is improved. In [10], a backstepping procedure is presented and formulated to realize a coupled longitudinal and lateral control in lane change or collision avoidance maneuvers. Kumarawadu et al. [11] synthesizes the combined lateral and longitudinal controller using a proportional plus derivative control coupled with an online adaptive neural module that acts as a dynamic compensator. But, it is worth mentioning that the tire coupled features are entirely ignored in these combined control approaches.

In particular, autonomous electric vehicles adopt the dynamic over-actuated or redundant structure to improve the reliability and availability of vehicles [12,13]. However, in a redundant vehicle system, it is difficult to determine an appropriate method to accurately translate the desired total forces/moment into tire lateral and longitudinal forces for each actuator [14].

In order to deal with the uncertain nonlinearities, strong coupling and over-actuated features of autonomous electric vehicles, this paper presents an adaptive hierarchical control framework for coordinating the lateral and longitudinal dynamics of vehicles, this proposed approach not merely insures that the tracking deviation and system states can asymptotically converge to the desired values, but also accomplish the reconfiguration and allocation of the redundant tire actuators. The main contributions of this paper are as follows.

I. An adaptive hierarchical control framework for coor-dinating the lateral and longitudinal motion of autonomous distributed electric vehicles in a formation is established.
II. A NN-based adaptive high-level controller is devel-oped to deal with the uncertain and nonlinear features, the closed-loop stability issues of proposed high-level control law are ensured through the Laypunov-based theorem.
III. The presented dynamic coordinated low-level con-trol law consists of a SQP control allocation law and the wheel slip ratio/ sideslip angle regulators, which can effec-tively manage the tire redundant actuators within the physi-cal constraints.

The rest of this paper is organized as follows. Section 2 provides a nonlinear vehicle dynamic model in a formation is established. Section 3 presents a NN-based adaptive backstepping high-level control law to deal with the uncer-tain and nonlinear features of autonomous electric vehicles. Section 4 presents a dynamic coordinated low-level control law for managing the over-actuated tire actuators. Section 5 evaluates the effectiveness of the proposed control scheme. Finally, Section 6 concludes this paper.

System Descriptions

Vehicle Dynamic Model

Autonomous distributed electric vehicles are multi-input multi-output nonlinear mechanical systems. Newton-Euler equations governing the dynamics of autonomous distributed electric vehicles under the influence of external torques and forces are shown in Fig.1. A simplified vehicle dynamic model can be obtained as follows

$$\dot{q} = A(q) + BF + \xi \tag{1}$$

where

$$A(q) = \begin{bmatrix} v_y r - F_{ax} - F_r \\ -v_x r - F_{ay} \\ 0 \end{bmatrix}; B = \begin{bmatrix} 1/m & 0 & 0 \\ 0 & 1/m & 0 \\ 0 & 0 & 1/I_z \end{bmatrix}$$

$q = [v_x\ v_y\ r]^T$ is the state vector, $F = [F_x\ F_y\ M_z]^T$ is the input vector, $\xi = [\xi_x\ \xi_y\ \xi_r]^T$ is the disturbance vector. v_x and v_y denote the lateral and longitudinal velocities, respectively. r is the yaw rate. m denotes the total mass of vehicle, I_z is the yaw inertia, c_a is the aero dynamical coefficient. ξ_x, ξ_y and ξ_r denote the uncertainties and external disturbances caused by the unmodeled dynamics and time-varying parameters. F_X, F_Y and M_Z represent the total forces and moment acting on vehicles, respectively, which can be written as follows

$$F_x = \sum_{i=1}^{2} F_{xi}\cos\delta_i + \sum_{i=3}^{4} F_{xi} - \sum_{i=1}^{2} F_{yi}\sin\delta_i$$

$$F_y = \sum_{i=1}^{2} F_{xi}\sin\delta_i + \sum_{i=1}^{2} F_{yi}\cos\delta_i + \sum_{i=3}^{4} F_{yi}$$

$$M_z = \sum_{i=1}^{2} l_f F_{xi}\sin\delta_i + \sum_{i=1}^{2} l_f F_{yi}\cos\delta_i - \sum_{i=3}^{4} l_r F_{yi} + \sum_{i=1}^{2}(-1)^i \frac{d_f}{2} F_{xi}\cos\delta_i - \sum_{i=3}^{4}(-1)^i \frac{d_r}{2} F_{xi} + \sum_{i=1}^{2}(-1)^i \frac{d_f}{2} F_{yi}\sin\delta_i \tag{2}$$

where F_{xi} and F_{yi} are the tire longitudinal and lateral forces, respectively. l_f and l_r are the distances from CG to the front and rear axles. d_f and d_r are the front and rear wheel treads, respectively. δ_i denotes the wheel steering angle.

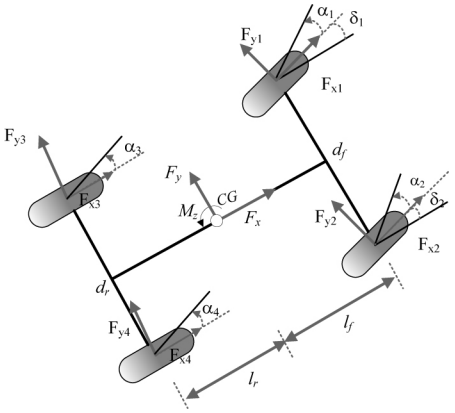

Figure 1. Distributed electric vehicle dynamic model

If the rolling resistance and the tire deformation are neglected, the rotational dynamics of each wheel is modeled as

$$J_\omega \dot{\omega}_i = T_{\omega i} - F_{xi} R_\omega \tag{3}$$

where ω_i is the wheel angular velocity, $T_{\omega i}$ is the wheel torque, J_ω represents wheel moment of inertia about the axis of rotation, R_ω is the wheel effective radius.

In this paper, the dugoff tire model is used to describe the nonlinearities and the coupled tire slip features, which can be written as [15,16]

$$F_{xi} = C_{\lambda i} \frac{\lambda_{xi}}{1+\lambda_{xi}} f(D_i) \tag{4}$$

$$F_{yi} = C_{\alpha i} \frac{\tan(\alpha_i)}{1+\lambda_{xi}} f(D_i) \tag{5}$$

$$f(D_i) = \begin{cases} (2-D_i)D_i, & if\ D_i < 1 \\ 1, & if\ D_i \geq 1 \end{cases} \tag{6}$$

where $C_{\lambda i}$ and $C_{\alpha i}$ represent the tire longitudinal and lateral stiffnesses, respectively. D_i provides the tire operating region, which is calculated as

$$D_i = \frac{\mu F_{zi}(1+\lambda_{xi})}{2\sqrt{(C_{\lambda i}\lambda_{xi})^2 + (C_{\alpha i}\tan(\alpha_i))^2}} \tag{7}$$

where μ is the tire-road friction coefficient,

The wheel slip angle α_i and slip ratio λ_{xi} are defined as

$$\alpha_i = \delta_i - \tan^{-1}\left(\frac{v_y + l_f r}{v_x \pm \frac{d_f}{2} r}\right) \quad \text{for} \quad i = 1,2 \tag{8}$$

$$\alpha_i = -\tan^{-1}\left(\frac{v_y - l_f r}{v_x \pm \frac{d_f}{2} r}\right) \quad \text{for} \quad i = 3,4 \tag{9}$$

$$\lambda_{xi} = \begin{cases} \frac{R_\omega \omega_i}{v_i \cos\alpha_i} - 1 & v_i \cos\alpha_i \geq R_\omega \omega_i \\ 1 - \frac{v_i \cos\alpha_i}{R_\omega \omega_i} & v_i \cos\alpha_i < R_\omega \omega_i \end{cases} \tag{10}$$

where v_i is the wheel velocity.

Kinematic Model

Figure 2 illustrates the kinematic structure about a formation of multiple autonomous electric vehicles on a lane in intelligent transportation system. From the configuration of a formation, the resulting kinematic model can be written as

$$\dot{\boldsymbol{e}} = \begin{bmatrix} \dot{e}_x \\ \dot{e}_y \\ \dot{e}_\alpha \end{bmatrix} = \begin{bmatrix} v_p - v_x - \tau_h \dot{v}_p \\ v_x e_\alpha - v_y - r D_L \\ v_x K_L - r \end{bmatrix} \tag{11}$$

where e_x is the spacing deviation between the leader and the follower vehicles, e_y and e_a are the lateral and angular deviations between the vehicles and the reference trajectory, respectively. v_p is the longitudinal velocity of the leader vehicle, τ_h is the headway, d_0 is a fixed stopping offset value. K_L is the curvature of reference trajectory, D_L is the specified look-ahead distance, which is a major factor on the influence of the control system performance [17, 18].

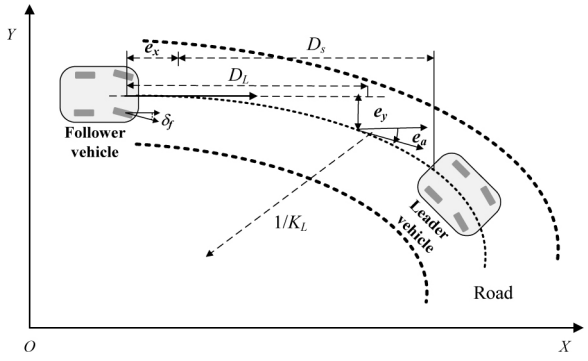

Figure 2. Vehicle kinematics in a formation

Coordinated Control Framework

The mission of coordinated lateral and longitudinal dynamic control for autonomous distributed electric vehicles in a formation is to guarantee that the autonomous distributed electric vehicles travel in the same reference trajectory at the same speed with the desired inter-vehicle distances, while insuring the system performances of safety, stability and riding comfort. However, the design of coordinated control approach for autonomous distributed electric vehicles faces two major challenges such as: I) Autonomous distributed electric vehicles have the properties of uncertain nonlinearities and strong coupling, the proposed control system should effectively overcome these dynamic features. II) Over-actuated tire actuators are equipped in the autonomous distributed electric vehicles to improve the reliability and maneuverability, the proposed control system should accurately handle with the redundancy of tire actuators.

To deal with the above two major challenges, a novel coordinated control system for managing the longitudinal and lateral dynamics of autonomous distributed electric vehicles in a formation is designed as shown in Figure 3. First, a neuro-network based adaptive backstepping high level total control law is constructed to determine the total forces and moment of autonomous distributed electric vehicles to achieve the desired states of vehicles. Then, a dynamic coordinated low-level control law is presented for accurately managing the redundant tire actuators in real time.

Adaptive Total High-Level Controller

In this section, to effectively supervise the system states and govern the vehicle planar motions, a NN-based adaptive backstepping high-level control law which contains three steps, is designed to generate the desired total forces and torque. At each step, the uncertainties and switching function terms of backstepping sliding mode control law are adaptively adjusted using the neural networks [19, 20, 21]. The specific proposed high-level control law is described as follow.

Step 1

At this step, the control goal is to make the lateral error e_y approach to zero, the first error variable is defined as $s_{11}=e_y$. To facilitate the stability analysis, choosing a scalar function as $V_{11}=1/2s_{11}^2$, then, whose time derivative along s_{11} can be expressed as

$$\dot{V}_{11}=s_{11}\dot{s}_{11}=s_{11}\dot{s}_{11}=s_{11}(v_x e_a-v_y-rD_L) \tag{12}$$

In (12), the virtual control input is viewed as $v_x e_a$ - rD_L, it can be seen that, the error variable s_{11} is close to zero with a stability criteria that the time derivative of V_{11} is negative definite, such that $\dot{V}_{11}=-c_1 {s_{11}}^2\le 0$, c_1 is a positive constant. To achieve this stability criterion, the stabilization of s_{11} can be obtained by introducing a desired virtual control input value ζ_{d1}, which can be written as

$$\zeta_{d1}=v_y-c_1 s_{11} \tag{13}$$

Next, the second error variable s_{12} between the virtual control input $v_x e_a$-rD_L and its desired input value ζ_{d1} is given as

$$s_{12}=v_x e_a-rD_L-\zeta_{d1} \tag{14}$$

Substituting (14) into the formula $\dot{V}_{11}=s_{11}\dot{s}_{11}$, yields

$$\dot{V}_{11}=s_{12}s_{11}-k_1 s_{11}^2 \tag{15}$$

It is worth noting that if s_{12} is equal to zero then the inequality $\dot{V}_{11}=s_{11}s_{12}-c_1 s_{11}^2\le 0$ is satisfied with $\zeta_{d1}=v_y$ - $c_1 s_{11}$.

Defining the second scalar function candidate as

$$V_{12}=V_{11}+\frac{1}{2}{s_{12}}^2 \tag{16}$$

The time derivative of V_{12} can be obtained as

$$\dot{V}_{12}=\dot{V}_{11}+s_{12}\dot{s}_{12}=-c_1 s_{11}^2-s_{11}s_{12}+s_{12}\dot{s}_{12} \tag{17}$$

Choosing the backstepping sliding mode control law of lateral deviation as

$$u_1=-c_2 s_{12}-s_{11}-v_y r e_a+f_1(e,q)-v_x e_a-v_x r-\chi_1\,\mathrm{sgn}(s_{12}) \tag{18}$$

where χ_1 is a positive constant.

Thus, the formula (19) is true, as follows

$$\dot{V}_{12}=-c_1 {s_{11}}^2-c_2 {s_{12}}^2 \tag{19}$$

where c_2 is a positive constant.

However, since the function $f_1(e,q)$ is unknown and uncertain, the desired control law cannot be availably implemented in practice, meanwhile, the control law (18) is usually discontinuous, which can lead to a high frequency chatting phenomenon near the sliding mode surface.

In order to availably handle with the issues of uncertainties and chatting phenomenon of vehicle control system, a NN-based adaptive backstepping control law is designed as:

$$u_1=-c_2 s_{12}-s_{11}-v_y r e_a+\hat{f}_1(e,q)-v_x e_a-v_x r+\hat{\chi}_1 \tag{20}$$

where the uncertain term $\hat{f}_1(e,q)$ and the variable structure term $\hat{\chi}_1$ are approximated by neuro networks as follows

$$\hat{f}_1(e,q)=\hat{W}^T h_1(e,q)\,;\ \hat{\chi}_1=\hat{\theta}^T\phi(s_{12}) \tag{21}$$

$$\tilde{f}_1=f_1-\hat{f}_1=W_1^{*T}h_1+\varepsilon_{h1}-\hat{W}_1^T h_1=\tilde{W}_1^T h_1+\varepsilon_{h1} \tag{22}$$

$$\tilde{\chi}_1=\chi_1-\hat{\chi}_1=\theta_1^{*T}\phi_1+\varepsilon_{\phi 1}-\hat{\theta}_1^T\phi_1=\tilde{\theta}_1^T\phi_1+\varepsilon_{\phi 1} \tag{23}$$

In order to guarantee the stability of control system, choosing the adaptive control law as

$$\dot{\hat{W}}_1=-\gamma_1 s_{12}h_1(e,q)\,;\ \dot{\hat{\theta}}_1=-\mu_1 s_{12}\phi_1(s_{12}) \tag{24}$$

where γ_1 and μ_1 are positive constants.

Step 2

This step aims to regulate the angular deviation of autonomous distributed electric vehicles, by introducing the following error variable s_{21} as

$$s_{21}=e_a \tag{25}$$

Defining the third scalar function as $V_3=1/2s_{21}^2$, then, the time derivative of V_3 along s_{21} is given as

$$\dot{V}_{21}=s_{21}\dot{s}_{21}=s_{21}(v_x D_L-r) \tag{26}$$

In equation (26), by viewing $v_x D_L$ as a virtual control input, and the condition for which s_{21} approach to zero is that $\dot{V}_{21}$ must be negative definite such as $\dot{V}_{21}=-c_3 s_{21}^2\le 0$, c_3 is a positive constant, therefore, the desired virtual control input ζ_{d2} can be obtained as

$$\xi_{d2} = r - c_3 s_{21} \tag{27}$$

Defining the regulating error variable s_{22} between the virtual control input $v_x D_L$ and its desired value ξ_{d2} as

$$s_{22} = v_x D_L - \xi_{d2} \tag{28}$$

Substituting $v_x D_L = s_{22} + \xi_{d2}$ into $\dot{V}_3 = s_{22}\dot{s}_{22}$, yields

$$\dot{V}_{21} = -s_{21}s_{22} - c_3 s_{21}^2 \tag{29}$$

Obviously, it can be seen that $\dot{V}_{21} = -s_{21}s_{22} - c_3 s_{21}^2 \le 0$ is satisfied only when s_{22}=0, therefore, next step is necessary.

Choosing the fourth scalar function as

$$V_{22} = V_{21} + \frac{1}{2}s_{22}^2 \tag{30}$$

The time derivative of (30) is obtained as

$$\dot{V}_{22} = \dot{V}_{21} + s_{22}\dot{s}_{22} = -c_3 s_{21}^2 - s_{21}s_{22} + s_{22}\dot{s}_{22} \tag{31}$$

Choosing the control law with regard to angular deviation as

$$u_2 = -c_4 s_{22} - s_{21} - v_y r D_L + \hat{f}_2(e,q) - c_4 s_{22} \tag{32}$$

Then, the following formula (33) is true.

$$\dot{V}_{22} = -c_3 s_{21}^2 - c_4 s_{22}^2 \tag{33}$$

Hence, a NN-based adaptive backstepping control law of angular deviation is obtained as:

$$u_2 = -c_4 s_4 - s_{21} - v_y r D_L + \hat{f}_2(e,q) - c_4 s_{22} + \hat{\chi}_2 \tag{34}$$

with

$$\hat{f}_2(e,q) = \hat{W}_2^T h_2(e,q)\ ;\ \hat{\chi}_2 = \hat{\theta}^T \phi_2(s_{22}) \tag{35}$$

$$\tilde{f}_2 = f_2 - \hat{f}_2 = W_2^{*T} h_2 + \varepsilon_{h2} - \hat{W}_2^T h_2 = \tilde{W}_2^T h_2 + \varepsilon_{h2} \tag{36}$$

$$\tilde{\chi}_2 = \chi_2 - \hat{\chi}_2 = \theta_2^{*T}\phi_2 + \varepsilon_{\phi 2} - \hat{\theta}_2^T \phi_2 = \tilde{\theta}_2^T \phi_2 + \varepsilon_{\phi 2} \tag{37}$$

Choosing the adaptive law as

$$\dot{\hat{W}}_2 = -\gamma_2 s_{22} h_2(e,q)\ ;\ \dot{\hat{\theta}}_2 = -\mu_2 s_{22}\phi_2(s_{22}) \tag{38}$$

where γ_2 and μ_2 are positive constants.

Step 3

The final control law with regard to the adjustment of longitudinal deviation will be derived as this step. Defining the error variable s_{31} as

$$s_{31} = e_x \tag{39}$$

Choosing the fifth scalar Lyapunov function as $V_{31} = 1/2 s_{31}^2$, and the time derivative of V_{31} is obtained as

$$\dot{V}_{31} = s_{31}\dot{s}_{31} = s_{31}(v_p - v_x - \tau_h \dot{v}_p) \tag{40}$$

In (40), the virtual control input is reviewed as v_x, the condition for which s_{31} approach to zero is that $\dot{V}_{31}$ must be negative definite such that $\dot{V}_{31} = -c_5 s_{31}^2 \le 0$, c_5 is a positive constant. Therefore, the desired virtual control ζ_{d3} can be obtained as

$$\xi_{d3} = v_p - \tau_h \dot{v}_p + c_5 s_{31} \tag{41}$$

Defining the error variable s_{32} between the virtual control v_x and its desired value ξ_{d3} as

$$v_x = s_{32} + \xi_{d3} \tag{42}$$

Substituting $v_x = s_{32} + \zeta_{d3}$ into $\dot{V}_{31} = s_{31}\dot{s}_{31}$, then

$$\dot{V}_{31} = -s_{31}s_{32} - c_5 s_{31}^2 \tag{43}$$

It can be seen that $\dot{V}_{31} = -s_{31}s_{32} - c_5 s_{31}^2 \le 0$ is satisfied only when s_{32}=0. Therefore, the next control objective is to search the control variables which make error variable s_{32} asymptotically converge to zero.

Choosing the sixth scalar function as

$$V_{32} = V_{31} + \frac{1}{2}s_{32}^2 \tag{44}$$

Its time derivative is

$$\dot{V}_{32} = \dot{V}_{31} + s_{32}\dot{s}_{32} = -c_5 s_{31}^2 - s_{31}s_{32} + s_{32}\dot{s}_{32} \tag{45}$$

Let

$$\frac{1}{m}F_x = -c_6 s_{32} - s_{32} + c_5 s_{31} - v_y r + \frac{c_a}{m}v_x^2 + v_p - \tau_h \dot{v}_p \tag{46}$$

Thus

$$\dot{V}_{32} = -c_5 s_{31}^2 - c_6 s_{32}^2 \le 0 \tag{47}$$

where c_6 is a positive constant.

The adaptive backstepping control law of longitudinal deviation using neuro networks is designed as

$$u_3 = -c_6 s_{32} - s_{32} + c_5 s_{31} - v_y r + \hat{f}_3(e,q) + v_p - \tau_h \dot{v}_p + \hat{\chi}_3 \tag{48}$$

with

$$\hat{f}_3(e,q) = \hat{W}_3^T h_3(e,q)\ ;\ \hat{\chi}_3 = \hat{\theta}_3^T \phi_3(s_{32}) \tag{49}$$

$$\tilde{f}_3 = f_3 - \hat{f}_3 = W_3^{*T} h_3 + \varepsilon_{h3} - \hat{W}_3^T h_3 = \tilde{W}_3^T h_3 + \varepsilon_{h3} \tag{50}$$

$$\tilde{\chi}_3 = \chi_3 - \hat{\chi}_3 = \theta_3^{*T} \phi_3 + \varepsilon_{\phi 3} - \hat{\theta}_3^T \phi_3 = \tilde{\theta}_3^T \phi_3 + \varepsilon_{\phi 3} \tag{51}$$

Choosing the following adaptive law as

$$\dot{\hat{W}}_3 = -\gamma_3 s_{32} h_3(e,q)\ ;\ \dot{\hat{\theta}}_3 = -\mu_3 s_{32} \phi_{32}(s_{32}) \tag{52}$$

where γ_3 and μ_3 are positive constants.

Through integrating the equations (18), (34) and (48), the adaptive backstepping high-level control law is obtained as

$$\begin{bmatrix} F_x \\ F_y \\ M_z \end{bmatrix} = \begin{bmatrix} a_{11} & a_{12} & a_{13} \\ a_{21} & 0 & a_{23} \\ a_{31} & 0 & 0 \end{bmatrix}^{-1} \begin{bmatrix} d_1 \\ d_2 \\ d_3 \end{bmatrix} \tag{53}$$

where

$$\begin{cases} d_1 = -c_2 s_{12} - s_{11} - v_y r e_a + \hat{f}_1 - v_x e_a - v_x r + \hat{\chi}_1 \\ d_2 = -c_4 s_{22} - s_{21} - v_y r D_L + \hat{f}_2 + \hat{\chi}_2 \\ d_3 = -c_6 s_{32} - s_{31} + c_5 \dot{s}_{31} - v_y r + \hat{f}_3 + v_p - \tau_h \dot{v}_p + \hat{\chi}_3 \end{cases}$$

$$a_{11} = \frac{e_a}{m}; a_{12} = -\frac{1}{m}; a_{13} = -\frac{D_L}{I_z};$$

$$a_{21} = \frac{D_L}{m}; a_{23} = \frac{1}{I_z};\ a_{31} = \frac{1}{m}.$$

Dynamic Coordinated Low-Level Controller

Autonomous distributed electric vehicles adopt the over actuated tire actuators to meet fault tolerance and control reconfiguration requirements. Full utilization of the redundancy of tire actuators requires selection of a particular set of tire longitudinal and lateral forces from a finite dimensional space [22, 23]. In this section, primarily, a SQP control allocation strategy is proposed to optimally allocate the desired total forces and moment among all the four tire actuators within their respective physical constraints, then, an inverse tire model and two inner regulators for each wheel are designed to accurately track the desired wheel slip ratio and slip angle.

Total Forces/Moment Allocation

To overcome the coupled and over-actuated features of autonomous distributed electric vehicles in a formation, while ensuring all tire actuators jointly produce the resultant forces/torque specified by the NN-based adaptive backstepping high-level control law, a SQP control allocation approach is designed to manage the redundant tire actuators within the physical constraints. The resultant forces/torque F can be expressed in a linear function of the product of the tire forces u and the control effectiveness matrix M_f as follows

$$F = M_f u \tag{54}$$

with

$$u = \begin{bmatrix} F_x & F_y & M_z \end{bmatrix}^T \tag{55}$$

$$M_f = \begin{bmatrix} 1 & 0 & 1 & 0 & 1 & 0 & 1 & 0 \\ 0 & 1 & 0 & 1 & 0 & 1 & 0 & 1 \\ -\frac{d_f}{2} & l_f & \frac{d_f}{2} & l_f & -\frac{d_r}{2} & -l_r & \frac{d_r}{2} & -l_r \end{bmatrix} \tag{56}$$

$$u = \begin{bmatrix} F_{x1} & F_{y1} & F_{x2} & F_{y2} & F_{x3} & F_{y3} & F_{x4} & F_{y4} \end{bmatrix}^T \tag{57}$$

Based on the Karush-Kuhn-Tucker conditions, the control allocation of over-actuated tire actuators can be converted as a nonlinear program through optimizing the manipulated tire forces to realize the minimum control deviation and the energy consumption, which can be expressed as follows

$$\min_{u,v} u^T P u + v^T Q v \qquad \text{subject to} \begin{matrix} M_f u = F_d + v \\ Cu \geq U \end{matrix} \tag{58}$$

with

$$C = \begin{pmatrix} I \\ -I \end{pmatrix}; \qquad U = \begin{pmatrix} u_{\min} \\ -u_{\max} \end{pmatrix} \tag{59}$$

where P and Q are positive definite, which represent the corresponding weighting matrices. The weighting matrix Q should be much larger than P, which means $v \approx 0$, respectively. F_d is the desired force/moment, $\boldsymbol{v}$ is a vector of slack variables used to penalize $M_f u$ - F_d .The magnitude of the resultant friction forces of each tire should be less than its maximum available value, therefore, the interior of set is defined by the inequality constraints as

$$\Omega = \{u_i \in R^8 \,|\, u_{\min} \le u_i \le u_{\max},\ j = 1,...,8\ \}$$

(60)

It can be observed that the nonlinear program function (58) is convex. Defining the variable $z_i = [u_i^T, v_i^T]$,and introducing the rate constrain of actuator to ensure the real time performance of control allocation, the optimization problem (58) can be expressed as the sequential quadratic-programming (SQP) form, as follows

$$\begin{aligned} &z(t) = \arg\min_{z_i(t)} \{\left\| W_1 z(t) \right\|^2 + \left\| W_2 \left[z(t) - z(t-T) \right] \right\|^2 \} \\ &\text{subject to } Nz = F_d \end{aligned}$$

(61)

where z_i is the actual control input, W_1 and W_2 are symmetric weighting matrices, and $\|\cdot\|$ denotes the 2-norm.

Dynamic Regulator

A dynamic regulating mechanism is employed to achieve the desired tire lateral and longitudinal forces, which consists of an inverse tire model and two slip ratio/angle regulators for each wheel.

1) Inverse tire Model

In the inverse tire model, equations (4) ~ (6) are simultaneously solved in the reverse direction [24]. The input variables are the desired tire lateral and longitudinal forces determined by the above control allocation approach, meanwhile the output variables are the desired wheel slip ratio/angle [25]. In addition, the inequality constraints of inverse tire model can be obtained as follows

$$f(\lambda_{xi}) = \begin{cases} (2-\lambda_{xi})\lambda_{xi}, & \text{if } \dfrac{\mu F_{zi}}{2} < \sqrt{F_{xi}^2 + F_{yi}^2} \le \mu F_{zi}; \\ 1, & \text{if } \sqrt{F_{xi}^2 + F_{yi}^2} \le \dfrac{\mu F_{zi}}{2}. \end{cases}$$

(62)

The inverse tire dynamic model can be obtained by solving the equations (2) ~ (5) in the reverse direction as follows

$$\lambda_{xi,des} = \begin{cases} \dfrac{F_{xi}}{C_{\lambda i} - F_{xi}} & D \ge 1 \\ \dfrac{\mu^2 F_{xi} F_{zi}^2}{4 C_{\lambda i} R_i (\mu F_{zi} - R_i) - \mu^2 F_{xi} F_{zi}^2} & D < 1 \end{cases}$$

(63)

$$\alpha_{i,des} = \begin{cases} \operatorname{atan} \dfrac{F_{yi} C_{\lambda i}}{C_{\alpha i}(C_{\lambda i} - F_{xi})} & D \ge 1 \\ \operatorname{atan} \dfrac{\mu^2 F_{xi} F_{zi}^2}{4 C_{\lambda i} C_{ai} R_i (\mu F_{zi} - R_i) - C_{ai} \mu^2 F_{xi} F_{zi}^2} & D < 1 \end{cases}$$

(64)

where $\lambda_{xi,d}$ and $\alpha_{i,des}$ are the desired wheel slip ratio and sideslip angle, respectively, F_{zi} is the tire normal force, $D = \dfrac{\mu F_{zi}}{2R_i}$ and $R_i = \sqrt{F_{xi}^2 + F_{yi}^2}$.

2) Wheel Slip Ratio Regulator

owing to the fact that the dynamic characteristics of wheel slip ratio are different under the driving/braking operating conditions, two regulators of wheel slip ratio are designed via the dynamic surface control technique, and the sign of wheel slip ratio precisely determine which of two regulators should be employed in each time step. The required wheel torque is concluded as follows

$$T_{wi,des} = \begin{cases} \dfrac{v_i J_\omega}{R_\omega} \left\{ t_1 - K_{si}(s_{xi} - s_{xi,d}) \right\} & \textit{braking} \\ \dfrac{\omega_i J_\omega}{1 - s_{xi}} \left\{ t_2 - K_{si}(s_{xi} - s_{xi,d}) \right\} & \textit{driving} \end{cases}$$

(65)

With

$$\begin{cases} t_1 = \dfrac{\dot{v}_i}{v_i}(1 - \lambda_{xi}) + \dfrac{R_\omega^2 F_{xi}}{v_i J_\omega} + s_{xi,d} \\ t_2 = \dfrac{\dot{v}_i}{R_\omega \omega_i} + \dfrac{(1 - \lambda_{xi})}{\omega_i J_\omega} F_{xi} R_\omega + \dot{s}_{xi,d} \end{cases}$$

where $K_{si} \in R^+$ is a positive constant, $T_{wi,des}$ is the desired wheel torque.

3) Tire Slip Angle Regulator

the wheel steering angle can be considered as an expression in terms of slip angles. Here, a proportional regulating law is applied to manage the slip angle for each wheel according as

$$\delta_{i,\text{des}} = K_i(\alpha_{i,\text{des}} - \alpha_i)$$

(66)

Where K_i for i=1,2 is the proportional gain,. $\delta_{i,\text{des}}$ and $\alpha_{i,\text{des}}$ are the desired wheel steering angle and slip angle,respectively.

Simulation Results

To evaluate the effectiveness of the proposed control approach, a series of Matlab-Adams cosimulation tests under different driving conditions are carried out, and the multi-body fourth degrees-offreedom nonlinear dynamics model of autonomous electric vehicles are established in Adams soft.

The goal of formation control is to keep a safe distance between the leader and follower vehicles while suppressing the location deviations of the vehicles relative to the desired trajectory. Figure 3 demonstrates the road curvature of reference trajectory and preceding acceleration of vehicles, it can be seen that the road curvature is instantaneous when entering a new curve. The initial longitudinal, lateral and angular deviations are set as 0.3m, 0.04rad and 0.4m, respectively. Besides, the initial speed of vehicle is set as 80km/h.

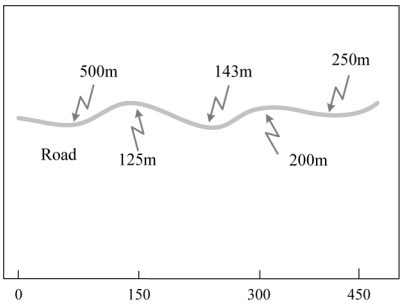

a.

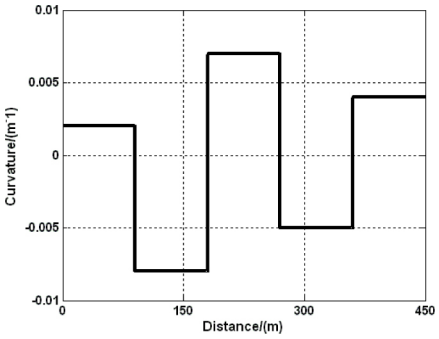

b.

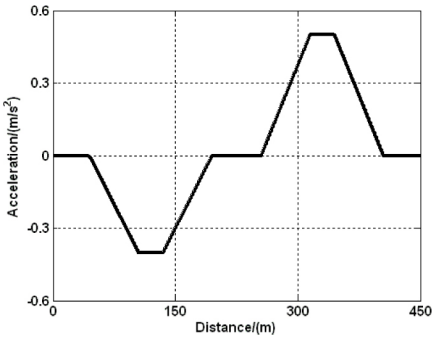

c.

Figure 3. Reference road and acceleration

Figure 4 illustrates the dynamic performances of proposed control system. The response results of longitudinal deviations are shown in Figure 4(a), it can be observed that the steady-state longitudinal deviations controlled by the proposed control approaches are 0m. In addition, Figure 4(a) indicates that the proposed control approach not only ensure the longitudinal deviation rapidly converge to zero, but also efficiently restrain the influences produced by the instantaneous road curvature. Figure 4(b) shows the dynamic responses of lateral deviation, it can be seen that the bounded convergence of steady-state lateral deviations can be ensured by the proposed control approach, besides, the maximum steady-state lateral error is generated in the road section with the largest curvature, the steady-state lateral error of the proposed control strategy are within ±0.08m, Figure 4(c) shows the dynamic responses of angular error, it can be seen that the proposed control approach can make the steady-state angular error be bounded by ±0.02rad.

Figure 4(d) describes the dynamic responses of sideslip angles, it can be seen that the sideslip angles controlled by the proposed control approach are only within a range of ±0.03rad. Furthermore, it is interesting to known that the proposed control system has low overshoot and small oscillation. It demonstrates that the proposed control system can make the sideslip angles within the desired range.

Figure 4(e) shows the response results of lateral velocity, it can be observed that the proposed control approach can limit the lateral velocity within ±0.05m/s, and the maximum lateral velocity occurs on the road with maximum curvature,the proposed control strategy can bring a good dynamic performance of lateral velocity .

The dynamic responses of yaw rates are shown in Figure 4(f), it is worth to note that the yaw rate can quickly converge to the desired states, and the proposed control system can effectively decrease the overshoot and improve the response speed.

Figure 4 shows that the proposed control system guarantees that the states of the closed-loop system globally asymptotically converge to zero and all closed-loop signals are uniformly bounded. Besides, the response results manifest that the proposed control approach can effectively improve the overall performances of the precision, stability, and riding comfort of automatic distributed electric vehicles.

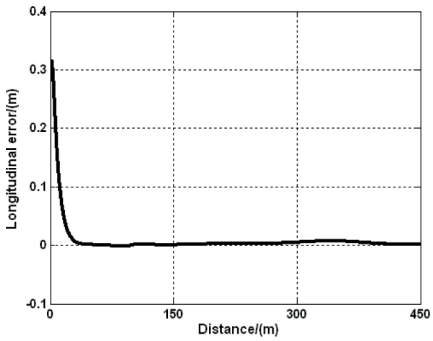

a.

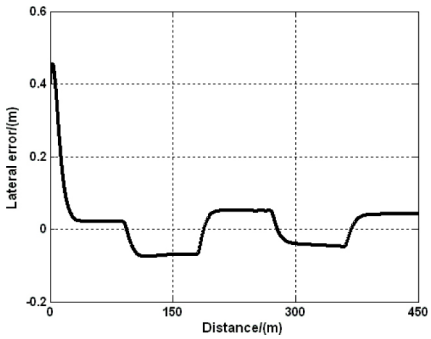

b.

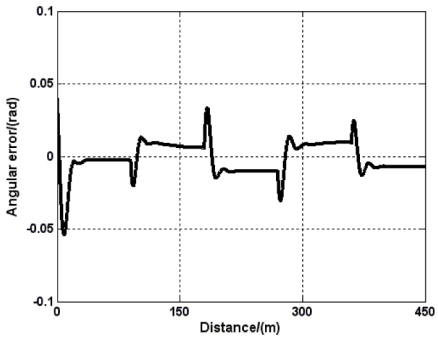

c.

Figure 4. Response results of system states

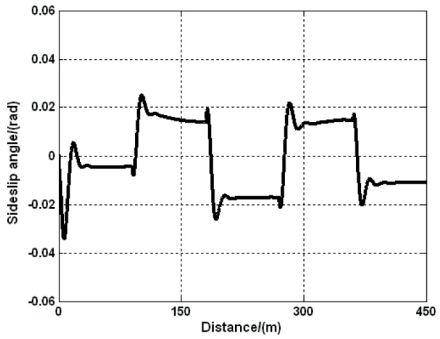

d.

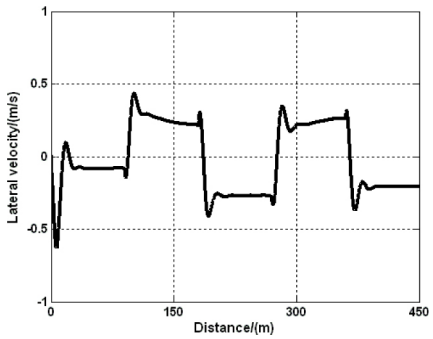

e.

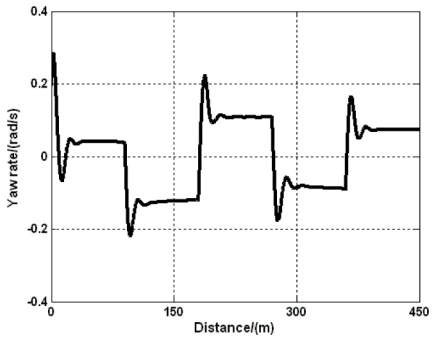

f.

Figure 4. (cont.) Response results of system states

The dynamically allocated results of tire longitudinal and lateral forces are shown in Figure 5. In order to ensure the achievement of automatic steering when vehicles moving in the curve with small curvature during the 0m~90m section of highway, the lateral forces for each wheel should be allocated is about 500N. During the 60m~380m section of highway, the maximum tire longitudinal and lateral forces are generated about 500N and1000 N, respectively, it can guarantee that the vehicles accelerate or decrease in the curves with the curvature. Finally, it is interesting to known that the smaller allocated tire longitudinal and lateral forces for each wheel ensure the driving stability of autonomous distributed electric vehicles. Figure 6 illustrates that the proposed control allocation law can real-time achieve the allocation and reconfiguration of the redundant tire actuators.

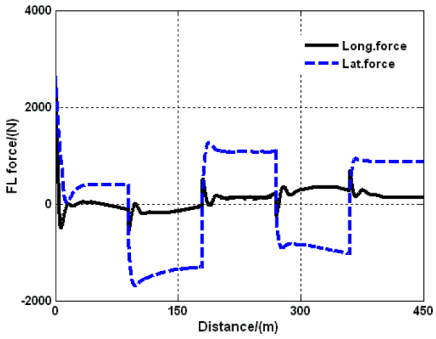

a.

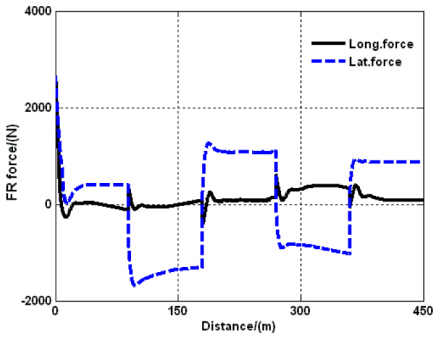

b.

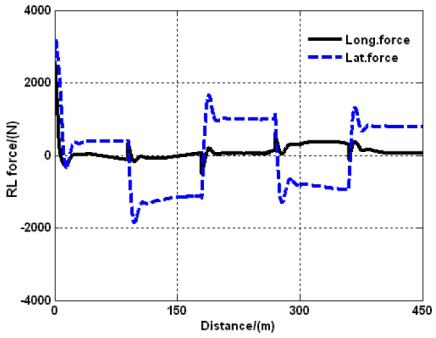

c.

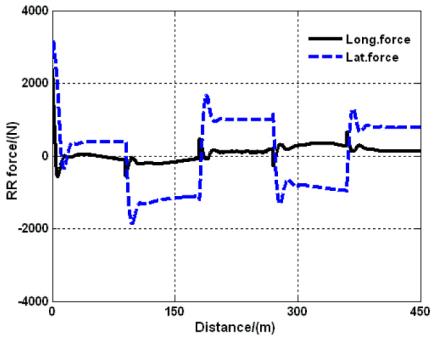

d.

Figure 5. Tire forces provided by the control allocation

Conclusions

To overcome the uncertain nonlinear, strong coupled and over-actuated properties of autonomous distributed electric vehicles in a formation, this paper presents an adaptive hierarchical coordinated control system to dynamically manage the longitudinal and lateral dynamics of vehicles. Primarily, an adaptive backstepping high level control law is designed to insure the tracking deviations and vehicle states asymptotically converge to the desired values, and the uncertain and switching function terms of high level control law are adjusted by neural net-works in real-time. Then, a dynamic coordinated low level control law is constructed, which is composed

of a control allocation law and two dynamic regulators for each wheel. The SQP control allocation law is used to achieve the allocation and reconfiguration of the over-actuated tire actuators, meanwhile, the saturation limits of tire actuators are taken into account. An inverse tire model is deduced to convert the desired tire forces to the desired wheel slip ratio/angle. Two wheel slip ratio/angle regulators in the low level controller are activated to track the desired wheel slip ratio/angle. The simulation results manifest that the proposed adaptive control scheme can effectively deal with the strong coupled and over-actuated features, and greatly improve the tracking performances of autonomous distribution electric vehicles in a formation.

References

1. Li Ke Q, Chen T, Luo Yu G, et al, Intelligent environment-friendly vehicles: Concept and Case Studies. IEEE Trans Intell Transp Syst, 2012, 13:318-328
2. Assad A, Ather G, Karl J, et al. Guaranteeing safety for heavy duty vehicle platooning: safe set computations and experimental evaluations. Control Eng Pract, 2014, 24:33-41
3. Ploeg J, Wouw N, Nijmeijer H. Lp string stability of cascaded systems: application to vehicle platooning. IEEE Trans Control Syst Tech, 2014, 22:786-793
4. Khalid E, Ghani D, Giri F et al. Nonlinear cascade strategy for longitudinal control of electric vehicle. J Dyn Syst-T ASME, 2014, 136:2877-2883
5. Ali G, Reza K, Shahram A. Stable decentralized control of a platoon of vehicles with heterogeneous information feedback. IEEE Trans Veh Tech,2013,62:4299-4308
6. Yue W,Guo G, Wang L, et al. Nonlinear platoon control of Arduino cars with range-limited sensors, Int J control, 2015, 88: 1037-1050
7. Zhou H, Saigal R, Dion F, et al. Vehicle platoon control in high-latency wireless communications environments. J Transp Res Rec, 2012, 10:81-90
8. Rachid A, Rodolfo O, Michel B. Combined longitudinal and lateral control for automated vehicle guidance. Vehicle Syst Dyn, 2014, 52:261-279
9. Song, P., Zong, C., and Tomizuka, M., "Combined Longitudinal and Lateral Control for Automated Lane Guidance of Full Drive-by-Wire Vehicles," *SAE Int. J. Passeng. Cars - Electron. Electr. Syst.* 8(2):419-424, 2015, doi:10.4271/2015-01-0321.
10. Lamri N, Lydie N. Backstepping based approach for the combined longitudinal-lateral vehicle control, In: Intelligent Vehicle Symposium, 2012, 395-400.
11. Kumarawadu S, Lee T. Neuroadaptive combined lateral and longitudinal control of highway using RBF networks. IEEE Trans Intell Trans Syst.2006, 7:500-511.
12. Castro R, Tanelli M, Rui E. Design of safety-oriented control allocation strategies for over-actuated electric vehicles. Vehicle Syst Dyn, 2014, 52:1017-1046.
13. Casavola R, Garone E. Fault-tolerant adaptive control allocation schemes for over-actuated systems. Int J Robust and Nonlin, 2012, 20:1958-1980.
14. Guo J, Luo Y, Li K. Dynamic coordinated control for over-actuated autonomous electric vehicles with nonholonomic constraints via nonsingular terminal sliding mode technique. Nonlinear Dynam, 2016, 3:1-15.
15. Bakker, E., Pacejka, H., and Lidner, L., "A New Tire Model with an Application in Vehicle Dynamics Studies," SAE Technical Paper 890087, 1989, doi:10.4271/890087.
16. Rajamani ~R. Vehicle dynamics and control 2nd Ed Berlin: Springer, 2012.
17. Guo J, Hu P, Li L, et al. L. Design of automatic steering controller for trajectory tracking of unmanned vehicles using genetic algorithms. IEEE Trans Veh Technol, 2012,61:2913-2924
18. Guo J, Li L, Li, K et al. An adaptive fuzzy sliding lateral control strategy of automated vehicles based on vision navigation. Vehicle Syst Dyna, 2013, 51:1502-1517.
19. Chen W, Jiao L, Li J, t al. Adaptive NN Backstepping output-feedback control for stochastic nonlinear strict-feedback systems with time-varying delays. IEEE T Syst Man Cy B, 2010, 40: 939-960.
20. Liu Y, Li T, Tao S, et al. Adaptive NN controller design for a class of nonlinear MIMO discrete-time system. IEEE T Neur Net Lear, 2015, 26:1007-1018.
21. Bin X. Robust adaptive neural control of flexible hypersonic flight vehicle with dead-zone input nonlinearity. Nonlinear Dyna, 2015, 80: 1509-1520
22. Johansen T, Fossen T. Control allocation-a survey. Automatica, 2013, 49:1807-1103
23. Li B, Du H, Li W, et al. Sideslip angle estimation based lateral dynamics control for omni-directional vehicles with optimal steering angle and traction/brake torque distribution. Mechatronics, 2015,30: 348-362
24. Guo J, Li K, Luo Y. Coordinated control of autonomous four wheel drive electric vehicles for platooning and trajectory tracking using a hierarchical architecture [J]. J Dyn Syst-T ASME, 2015, 137: 1-18
25. Wang R, Hu C, Wang Z, et al. Integrated optimal dynamics control of 4WD4WS electric ground vehicle with tire-road frictional coefficient estimation. Mech Syst Signal Pr,2015, 60: 727-741

Acknowledgments

This work was funded by the National Natural Science Foundation of China (No.61304193). Authors are grateful for helpful comments from referees to improve this manuscript.

The Engineering Meetings Board has approved this paper for publication. It has successfully completed SAE's peer review process under the supervision of the session organizer. The process requires a minimum of three (3) reviews by industry experts.

ISSN 0148-7191

http://papers.sae.org/2016-01-1875